

Received:
10 December 2020

Revised:
26 January 2021

Accepted:
08 February 2021

<https://doi.org/10.1259/bjr.20201423>

Cite this article as:

Kowa J-Y, Soneji N, Sohaib SA, Mayer E, Hazell S, Butterfield N, et al. Detection and staging of radio-recurrent prostate cancer using multiparametric MRI. *Br J Radiol* 2021; **94**: 20201423.

FULL PAPER

Detection and staging of radio-recurrent prostate cancer using multiparametric MRI

¹JIE-YING KOWA, FRCR, ¹NEIL SONEJI, FRCR, ¹S ASLAM SOHAIB, FRCR, ^{2,3}ERIK MAYER, PhD, FRCS, ⁴STEPHEN HAZELL, FRCPath, ¹NICHOLAS BUTTERFIELD, FRCR, ¹JOSHUA SHUR, FRCR and ¹DERFEL AP DAFYDD, FRCR

¹Department of Radiology, The Royal Marsden NHS Foundation Trust, 203 Fulham Road, Chelsea, London SW3 6JJ, UK

²Department of Surgery, The Royal Marsden NHS Foundation Trust, 203 Fulham Road, Chelsea, London SW3 6JJ, UK

³Department of Surgery & Cancer, St Mary's Hospital Campus, Imperial College London, Praed Street, London, W2 1NY, UK

⁴Department of Histopathology, The Royal Marsden NHS Foundation Trust, 203 Fulham Road, Chelsea, London SW3 6JJ, UK

Address correspondence to: Dr Jie-Ying Kowa

E-mail: k.jie-ying@nhs.net

Objective: We determined the sensitivity and specificity of multiparametric magnetic resonance imaging (MP-MRI) in detection of locally recurrent prostate cancer and extra prostatic extension in the post-radical radiotherapy setting. Histopathological reference standard was whole-mount prostatectomy specimens. We also assessed for any added value of the dynamic contrast enhancement (DCE) sequence in detection and staging of local recurrence.

Methods: This was a single centre retrospective study. Participants were selected from a database of males treated with salvage prostatectomy for locally recurrent prostate cancer following radiotherapy. All underwent pre-operative prostate-specific antigen assay, positron emission tomography CT, MP-MRI and transperineal template prostate mapping biopsy prior to salvage prostatectomy. MP-MRI performance was assessed using both Prostate Imaging-Reporting and Data System v. 2 and a modified scoring system for the post-treatment setting.

Results: 24 patients were enrolled. Using Prostate Imaging-Reporting and Data System v. 2, sensitivity, specificity, positive predictive value and negative predictive value was 64%, 94%, 98% and 36%. MP-MRI under staged recurrent cancer in 63%. A modified scoring system in which DCE was used as a co-dominant sequence resulted in improved diagnostic sensitivity (61%–76%) following subgroup analysis.

Conclusion: Our results show MP-MRI has moderate sensitivity (64%) and high specificity (94%) in detecting radio-recurrent intraprostatic disease, though disease tends to be under quantified and under staged. Greater emphasis on dynamic contrast images in overall scoring can improve diagnostic sensitivity.

Advances in knowledge: MP-MRI tends to under quantify and under stage radio-recurrent prostate cancer. DCE has a potentially augmented role in detecting recurrent tumour compared with the *de novo* setting. This has relevance in the event of any future modified MP-MRI scoring system for the irradiated gland.

INTRODUCTION

Following radical radiotherapy for prostate cancer, a proportion of patients develop biochemical recurrence (BCR). Post-radiotherapy BCR rates have been variably quoted at 21–54% in a recent systematic review.¹ Whilst serum prostate-specific antigen (PSA) assay is used to define BCR, elevated levels do not differentiate intra prostatic relapse from distant disease. Positron emission tomography/CT (PET/CT) with radio-labelled choline or prostate-specific membrane antigen tracer is a useful diagnostic tool in this regard: abnormal PET activity at sites of recurrence improves lesion localisation. Multiparametric magnetic resonance imaging (MP-MRI) offers superior spatial resolution of the prostate compared with PET/CT, therefore MP-MRI may be included in the imaging investigation of patients with BCR.

Certain alterations in the irradiated gland potentially complicate MRI analysis. After hormonal treatment, radiotherapy or a combination of both, the prostate reduces in size and exhibits generalised reduction in T2 signal intensity. This results in diminished zonal differentiation and contrast resolution between tumour and background parenchyma on T₂ weighted imaging (T₂WI).^{2–4} Diffusion-weighted imaging (DWI) and dynamic contrast enhanced (DCE) sequences may partly overcome these factors^{5,6}; however, treatment-related fibrosis also potentially affects lesion conspicuity on functional imaging.

In the *de novo* cancer setting, according to Prostate Imaging-Reporting and Data System v. 2 and 2.1 (PI-RADS v2/2.1), DWI is the dominant sequence in the peripheral

zone (the source of 70% of prostate cancer),⁷ with DCE playing a supplementary role in the overall scoring.^{8,9} The applicability of PI-RADS in the context of a previously treated gland is unclear, as are the relative advantages of DWI compared with DCE. Some authors suggest a greater role for DCE in the post-treatment setting compared with the *de novo* cancer setting.^{10,11}

Several studies have attempted to assess the diagnostic performance of DWI and DCE in radio-recurrent prostate cancer, using histopathological correlation with transrectal ultrasound-guided biopsy (TRUS-biopsy) as the reference standard.^{10–21} However, this biopsy technique is vulnerable to systematic error: the PZ may be oversampled, whereas the anterior, apical and midline regions are potentially undersampled.²² The seminal vesicles are also not routinely sampled. The use of TRUS-biopsy as reference standard is a significant limitation in these existing studies.

The diagnostic gold-standard is step-section analysis of whole-mount prostatectomy specimens. Limited published data exist on the diagnostic performance of MP-MRI using whole-mount pathological correlation, due to the small number of patients who are suitable candidates for salvage prostatectomy. Pucar et al²³ and Sala et al²⁴ correlated T_2 WI findings of radio-recurrent disease with pathological step-sections, but DWI and DCE sequences were not employed. To our knowledge, a study by Zattoni et al is the only one evaluating accuracy of multiparametric sequences against definitive pathology in radio-recurrent cancer.²⁵ The group utilised endorectal coils in their protocol, though body coil imaging remains the more common technique for MP-MRI.

Our primary objective is to assess diagnostic performance of MP-MRI [sensitivity, specificity, positive predictive value (PPV) and negative predictive value (NPV)] in detecting and staging radio-recurrent prostate cancer, using whole-mount histological correlation as the gold-standard. As proof of concept, the secondary objective is to assess for any incremental value of the DCE sequence in a modified diagnostic scoring system, as currently there is no formal reporting system designed specifically for evaluation of the irradiated gland.

PATIENTS AND METHODS

This was a retrospective study conducted at a single cancer centre, following institutional review board approval. Written informed consent was waived. Patients were identified over a 3-year period (2014–2017). All were cases of BCR following radical radiotherapy for prostate cancer. Eligible patients had MP-MRI for local assessment and staging, fluorine-18 PET/CT excluding distant disease, and transperineal template prostate mapping biopsy confirming local recurrence. Salvage prostatectomy was performed in those meeting eligibility criteria and who were assessed to be clinically fit for surgery.

Image acquisition

Imaging studies from several referring centres were included and MRI manufacturers varied accordingly. MP-MRI was performed on either 1.5 or 3.0 Tesla MRI scanners with a body coil. Essential sequences included small field of view axial T_2 WI, at least a second plane small field of view T_2 WI sequence, and DWI. DCE sequences were obtained after intravenous gadolinium; this was omitted in subjects with contraindications to gadolinium contrast. Suggested sequence parameters are provided in Table 1.

Surgery and histopathology

All prostatectomies were performed by a single uro-oncological surgeon with 10 years' experience. This involved robotically assisted salvage prostatectomy with wide local margins. The whole-mount prostatectomy specimens were reviewed by a single consultant urological histopathologist with over 10 years' experience. The histological report included these descriptors: tumour presence, volume, laterality, extra capsular extension (ECE), seminal vesicle involvement (SVI) and overall pathological staging (ypT stage). A Gleason score was not provided, as accurate tumour grading in the recurrence setting is confounded by treatment-related stigmata.

Image interpretation

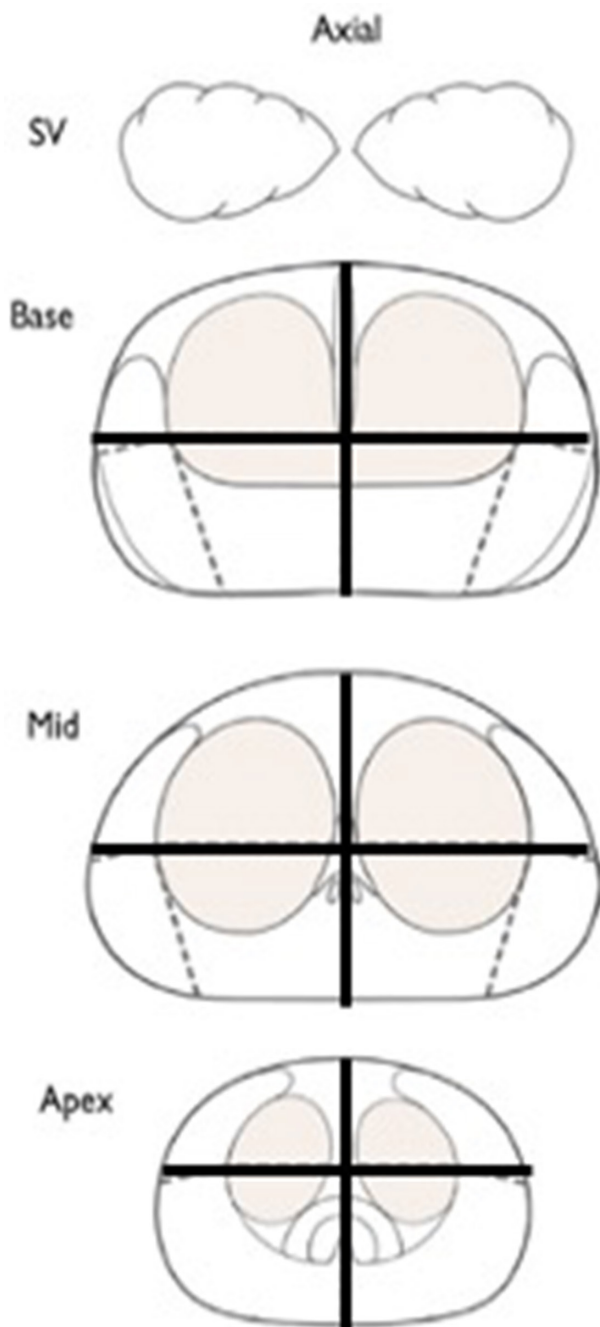
MR images were independently, retrospectively reviewed by two consultant radiologists with a special interest in prostate cancer imaging (one with 5 years' experience and one with over 10 years' experience). The readers were aware of the patients' previous

Table 1. Recommended technical parameters for 3.0 Tesla multiparametric-MRI sequences

Transverse large FOV T_1 W	TR/TE: 678/20 ms; section thickness 5 mm; intersection gap 1 mm; FOV 38 cm; matrix 320 × 320
Transverse large FOV T_2 W	TR/TE: 4370/108 ms; section thickness 5 mm; intersection gap 1 mm; FOV 38 cm; matrix 320 × 320
Large FOV DWI	TR/TE 10900/70 ms; section thickness 5 mm; intersection gap 0 mm; FOV 38 cm; matrix 320 × 320; B50, B600, B1050
High-resolution transverse T_2 W	TR/TE: 5500/77 ms; section thickness 5 mm; intersection gap 0 mm; FOV 17 cm; matrix 256 × 256
High-resolution coronal T_2 W	TR/TE: 6120/122 ms, section thickness 3 mm, intersection gap 0.3 mm; FOV 20 cm; matrix 320 × 320
Contrast sequence	TR/TE: 3.8/1.45 ms, section thickness 3 mm; intersection gap 0.6 mm; FOV 25 cm

DWI, diffusion-weighted imaging; FOV, field of view; TE, echo time; TR, repetition time; T_1 W, T_1 weighted; T_2 W, T_2 weighted.

Figure 1. Diagrams of the prostate on data collection forms



radiotherapy and BCR but blinded to further clinical information including prior MRI reports and histopathology results. Each study was read in this order: T_2 WI, high b-value DWI and apparent diffusion coefficient map, then DCE images (where available). Findings were recorded on data collection forms with diagrams of the prostate, prostatic capsule and seminal vesicles (Figure 1).

The readers graded diagnostic certainty for intra prostatic recurrence, ECE and SVI based on PI-RADS v. 2 criteria (the applicable iteration of PI-RADS at the time). Accordingly, appearances on T_2 WI and DWI were assigned a score from 1 to 5, DCE findings

– where available – were rated ‘negative’ or ‘positive’ and the prostates staged accordingly (Figures 2 and 3).

We undertook a subgroup analysis of patients who had the full complement of multiparametric sequences. In these patients, the readers recorded whether a lesion was better appreciated on DWI, DCE, or equally well-appreciated on both. In addition to binary values, the DCE was also assigned a numerical score from 1 to 5 (Figure 4) and given equal weight to DWI for PZ lesions and equal weight to T_2 WI for transition zone (TZ) lesions, generating a modified overall score (Figures 2 and 3).

Data analysis

For the purposes of statistical analysis, overall radiological scores of 1–3 were categorised ‘negative’ and scores of 4–5 categorised ‘positive’ for intraprostatic disease recurrence. Accordingly, each hemi-gland was designated disease ‘positive’ or ‘negative’ by PI-RADS v. 2 in all cases and additionally by the revised scoring system for the subgroup of patients.

MP-MRI scores were then cross-referenced with whole-mount prostatectomy findings as the reference standard. Radiological–pathological concordance was assessed on a per hemi-gland basis and the data set divided into histologically positive and negative regions for the calculation of sensitivity, specificity, PPV and NPV. MP-MRI detection of ECE and SVI was determined on a per-patient basis. Interobserver agreement was evaluated using unweighted K -values with MedCalc software and stratified according to Altman²⁶: a K -value of 0.20–0.40 was considered fair agreement, moderate when K ranged from 0.40 to 0.60, good when K ranged from 0.60 to 0.80, and very good when K was greater than 0.80.

RESULTS

A total of 24 patients were included in the study; all having had salvage prostatectomy for recurrent prostate cancer. Baseline characteristics are listed in Table 2. The scans were performed across 3 different centres: 22 at the hub institution, one at a medium-sized teaching hospital, and 1 at a district general hospital. Hub institution MP-MRIs were performed at 3.0 Tesla with small field of view T_2 WI in the axial and coronal planes and DWI; in four cases imaged at the hub an endorectal coil was also utilised, including the same sequences. The two external studies were performed at 1.5 Tesla, including axial and coronal small field of view T_2 WI, as well as DWI. All 24 studies were compliant with the essential sequences listed in the earlier section.

Histologically confirmed prostate cancer was present in 40 of 48 hemi-glands (83%). On a per-patient basis, 17 out of 24 subjects (71%) had bilateral disease and 6 out of 24 (25%) had unilateral disease. In one patient, there was no intraprostatic tumour, but the seminal vesicle was extensively infiltrated by tumour. Histologically confirmed ECE was identified in 21 of 24 patients (88%) and histologically confirmed SVI in 11 of 24 patients (46%).

Diagnostic performance according to PI-RADS v. 2 For detection and localisation of intraprostatic disease according to PI-RADS v. 2, the mean sensitivity, specificity, PPV and NPV

Figure 2. Peripheral Zone assessment with PI-RADS v. 2 and the revised scoring system. *Whichever is the highest scoring functional sequence. For example, if the DWI score is 5 and the DCE score is 1, the overall modified score is 5 (as in PI-RADS v. 2). If on the other hand the DWI score is 1 and the DCE score is 5, the overall modified score would also be 5 (whereas the PI-RADS v. 2 score would be 1. DCE, dynamic contrastenhanced; DWI, diffusion-weighted imaging; PI-RADS, Prostate Imaging-Reporting and Data System; T_2W , T_2 weighted.

Peripheral Zone (PZ)						
PI-RADS				Modified scoring		
DWI	T_2WI	DCE	PI-RADS score	*DWI or DCE	T_2WI	Modified score
1	Any	Any	1	1	Any	1
2	Any	Any	2	2	Any	2
3	Any	-	3	3	Any	3
		+	4			
4	Any	Any	4	4	Any	4
5	Any	Any	5	5	Any	5

values were 64%, 94%, 99%, 35% for both readers ($K = 0.67$; good interobserver agreement). The mean figures for ECE detection were 31%, 100%, 100%, 18% ($K = 0.48$; moderate agreement). For SVI, the mean values were 45%, 96%, 92%, 68% ($K = 0.75$; good agreement). A summary is provided in [Table 3](#).

Of the 24 patients, 15 (63%) were upstaged on histology (for both readers). None of the other nine cases were downstaged on histology with respect to Reader A. One of the remaining nine patients was down-staged from $\gamma T3b$ to $\gamma pT3a$ on histology with

respect to Reader B. Of the 24 patients, there were 21 cases with histologically confirmed extra prostatic extension ($\geq \gamma pT3a$). 12 (57%) of these were upstaged on histology from radiologically organ confined disease ($\leq \gamma T2c$).

Subgroup analysis of functional sequences

Intravenous gadolinium was contraindicated in seven patients due to renal insufficiency. 17 of 24 MP-MRI studies included both DWI and DCE. The sequence on which the lesion was best

Figure 3. Transition Zone assessment with PI-RADS v. 2 and the revised scoring system. **Whichever is the highest scoring sequence. For example, if the T_2WI score is 5 and the DCE score is 1, the overall modified score is 5 (as in PI-RADS v. 2). However, if the T_2WI score is 1 and the DCE score is 5, the overall modified score would also be 5 (whereas the PI-RADS v. 2 score would be 1. DCE, dynamic contrast enhanced; DWI, diffusion-weighted imaging; PI-RADS, Prostate Imaging-Reporting and Data System; T_2W , T_2 weighted; TZ, transition zone.

Transition Zone (TZ)						
PI-RADS				Modified scoring		
T_2WI	DWI	DCE	PI-RADS score	** T_2WI or DCE	DWI	Modified score
1	Any	Any	1	1	Any	1
2	Any	Any	2	2	Any	2
3	≤ 4	Any	3	3	≤ 4	3
	5		4			
4	Any	Any	4	4	Any	4
5	Any	Any	5	5	Any	5

Figure 4. DCE grading under the modified scoring system, adapted from PI-RADS v. 2. DCE, dynamic contrastenhanced; PI-RADS, Prostate Imaging-Reporting and Data System

DCE	Imaging characteristics
1	No early enhancement
2	Indistinct or linear/wedge shaped enhancement
3	Focal mild enhancement
4	Focal markedly hyperenhancing; <1.5 cm in greatest dimension
5	Focal markedly hyperenhancing; ≥1.5 cm in greatest dimension or definite extraprostatic extension/invasive behaviour

depicted was DWI in 4 of 17 (24%), and DCE in 9 of 17 (53%). Figure 5 is an example of better tumour depiction on DCE with respect to DWI. Lesion conspicuity was considered to be equivalent on DWI and DCE in 3 of 17 (18%) (example in Figure 6). In the remaining one case, disease was radiologically occult on MP-MRI, but histology revealed unilateral ypT3a cancer. In 2 of 17 patients (12%), the radiological diagnosis of SVI was only appreciable on DCE, being occult on DWI (example in Figure 7). These instances of radiological upstaging were all confirmed on whole mount histopathology.

Using a modified scoring system in which DCE was applied as a co-dominant sequence with respect to DWI and T₂WI (PZ and TZ lesions respectively), averaged across both readers, the sensitivity, specificity, PPV and NPV of detecting intra prostatic recurrence was 76%, 86%, 95%, 50% respectively (K = 0.57; moderate agreement). Details are provided in Table 4. With this MP-MRI scoring modification, 9 of 17 (53%) cases were upstaged from radiologically organ confined disease (<ypT2c) to histologically locally advanced disease (≥ypT3a).

Table 2. Patient characteristics

Characteristics (n = 24)	
Age, year (mean, range)	68.8 (58.5–77.0)
PSA before MP-MRI, ng/ml (median, IQR)	3.2 (2.3–5.2)
Interval between MP-MRI and surgery, days (median, IQR)	137.5 (84.5–177.3)
Pathological tumour stage	
ypT2a	2 (8%)
ypT2b	0 (0%)
ypT2c	1 (4%)
ypT3a	9 (38%)
ypT3b	11 (46%)
ypT4	1 (4%)
Pathological ECE	21 (88%)
Pathological SVI	11 (46%)

ECE, extracapsularenxtension; IQR, interquartile range; MP-MRI, multiparametric MRI; PSA, prostate specific antigen; SVI, seminal vesicle involvement.

DISCUSSION

To our knowledge, this is one of only two studies in which diagnostic performance of MP-MRI in local radio-recurrent prostate cancer was correlated against whole-mount prostatectomy specimens,²⁵ and the only one of those two studies which used standard body coil imaging. This histopathological gold-standard eliminates sampling error inherent in TRUS-biopsy, which is a significant confounder in most applicable literature on this subject.

In our study, locally recurrent disease tended to be extensive on whole mount pathology: bilateral in 71% (17/24) of patients and locally advanced (≥ypT3a) in 88% (21 of 24). Using PI-RADS v. 2, our study demonstrated a mean sensitivity and specificity of 64 and 94% for intraprostatic recurrent tumour, sensitivity and specificity of 31 and 100% for ECE, and sensitivity and specificity of 45 and 96% for SVI (Table 6). Specificity for all of these variables was very good. Although sensitivity for intraprostatic recurrence was fair (64%), sensitivity by PI-RADS v. 2 for ECE and SVI was poor at 31 and 45% respectively. With respect to PI-RADS v. 2, local recurrence was upstaged on histology in a substantial proportion of cases (63%, 15/24).

These results suggest that radio-recurrent disease tended to be underquantified and understaged on MP-MRI using PI-RADS v. 2, and this should be borne in mind when interpreting post-treatment imaging. This observation accords with study findings by Dinis Fernandes et al,²⁷ in which there was also a tendency to underestimate tumour size and extent on imaging.

In the few prior studies using gold-standard whole mount histological correlation, variable diagnostic performance of MRI is reported.^{23–25} Using PI-RADS v. 2, sensitivity for intraprostatic tumour detection in our study (mean 64%) was similar to Pucar et al (68%) but higher than Sala et al (mean 47%). Sensitivity for ECE in our study (mean 31%) was lower than Sala et al (mean 87%) and Zattoni et al (mean 61%). Sensitivity for SVI in our study (mean 45%) was similar to Sala et al (mean 50%) but lower than Zattoni et al (mean 69%).

Heterogeneity in study design may have contributed towards some of the larger variations in results. Although Pucar et al and Sala et al employed whole mount histology for radiological histological correlation, their MRI protocols were not multiparametric, as they did not include DWI or DCE sequences.

Table 3. Diagnostic performance of MP-MRI according to PI-RADS v. 2

	TP	FP	TN	FN	Sensitivity (%)	Specificity (%)
Intraprostatic disease, per hemi-gland (<i>n</i> = 48)						
Reader 1	22	0	8	18	55	100
Reader 2	29	1	11	7	73	88
Average					64	94
ECE, per patient (<i>n</i> = 24)						
Reader 1	5	0	3	16	24	100
Reader 2	8	0	3	13	38	100
Average					31	100
SVI, per patient (<i>n</i> = 24)						
Reader 1	5	0	13	6	45	100
Reader 2	5	1	12	6	45	92
Average					45	96

ECE, extracapsular extension; FN, false negative; FP, false positive; MP-MRI, multiparametric MRI; PI-RADS v. 2, Prostate Imaging-Reporting and Data System version 2; SVI, seminal vesicle involvement; TN, true negative; TP, true positive.

This constitutes a significant difference in methodology and, we would suggest, a significant strength in our study. Sala et al and Zattoni et al used endorectal coils to obtain images with higher signal-to-noise ratio; however, this technique is not commonly adopted in all centres due to patient discomfort and additional scan time incurred. This contrasts with our study, which was predominantly based on standard body coil imaging, and arguably produces more translatable results for real-world clinical practice. Statistical analyses in the study by Sala et al for the radiological assessment of ECE and SVI at the patient level were based on a lower threshold of suspicion; categorising scores of 1–2 as ‘positive’ and scores of 3–5 as ‘negative’. Given that a score of PI-RADS 3 indicates an indeterminate finding, we did not consider this score to fairly reflect ‘positivity’ for tumour detection and we therefore used a score threshold of ≥ 4 .

Interobserver agreement in our study for intraprostatic disease detection using PI-RADS v. 2 was moderate ($K = 0.57$), which may be due to the less familiar imaging context and lack of dedicated

reporting guidance for the treated prostate gland. In the *de novo* setting, applying PI-RADS v. 2 criteria and a score threshold of ≥ 4 for intraprostatic disease appears to generate better interobserver agreement. Rosenkrantz et al report moderate agreement of $K = 0.552$,²⁸ Girometti et al and Kassel-Seibert et al demonstrate good agreement of 0.63 and 0.68,^{29,30} whilst Park et al and Purysko et al quote very good values of 0.801 and 0.91 respectively.^{31,32}

In the subgroup of 17 patients who had both DWI and DCE imaging performed, DCE was most often the sequence on which lesions were considered to be better depicted. Lesions were considered better depicted on DCE in 53% (9/17) of cases, on DWI in 24% (4/17) of cases and equally well depicted on DCE and DWI in the remaining 18% (3/17). These findings support the assertion that DCE has a potentially greater role in the detection of locally recurrent prostate cancer than it does in the detection of *de novo* prostate cancer.^{9,10} Post-radiation fibrosis demonstrates ‘low and slow’ enhancement, whilst tumour foci are hypervascular and typically show early enhancement.^{33,34} It

Figure 5. Role of DCE, peripheral zone: A recurrence in the posteromedial peripheral zone of the right mid-gland is subtle on the high b-value DWI (A) and ADC sequences (B) but very conspicuous as an enhancing nodule on DCE image (arrowed in C). ADC, apparent diffusion coefficient; DCE, dynamic contrast enhanced; DWI, diffusion-weighted imaging.

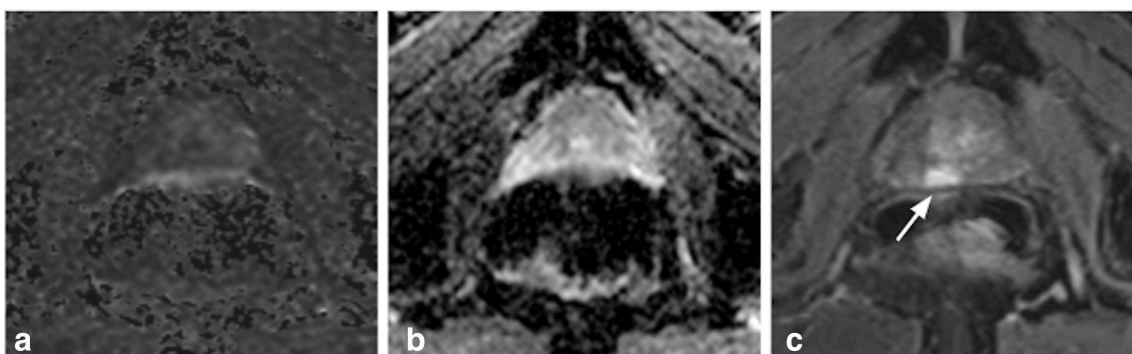


Figure 6. DWI and DCE, equally good: recurrence in the left anterior peripheral zone of the apex is equally well appreciated as a nodule that is hyperintense on high b-value image and hypointense on ADC (A + B, dashed arrows) with early enhancement on DCE (C, solid arrow). ADC, apparent diffusioncoefficient; DCE, dynamic contrast enhanced; DWI, diffusion-weighted imaging



may be that background radiation-induced parenchymal fibrosis has a more confounding effect on T_2 WI and DWI sequences than it does on DCE sequences.

Given the potential added value of DCE in assessing the irradiated prostate, we explored the feasibility of a corresponding modification to the overall MP-MRI scoring in which DCE was applied as a co-dominant sequence. This scoring modification led to improved sensitivity of intraprostatic tumour detection with respect to PI-RADS v. 2 (mean sensitivity 76 vs 61%). This gain in sensitivity was at the expense of a small reduction in the specificity compared with PI-RADS v. 2 (mean specificity 86 vs 93%) as the scoring modification resulted in a single false-positive case. The statistical effect of this was magnified due to the small number (8/48) of pathologically negative hemi-glands in our patient sample. Despite this, specificity for intraprostatic tumour detection using the scoring modification remained high. DCE therefore has a potentially augmented role in the assessment of recurrent disease compared with the *de novo* prostate cancer setting. A greater emphasis on DCE in the evaluation of suspected local radio-recurrent prostate cancer may aid targeted biopsy, case selection for salvage surgery and surgical planning. DCE may be particularly beneficial in situations where DWI is disproportionately distorted by artefact, *e.g.* from hip prostheses or brachytherapy seeds. Clearly, a formalised scoring system

intended for the treated prostate would be contingent upon a consensus statement from the PI-RADS working group, with assigned appropriate nomenclature (*e.g.* yPI-RADS).

Although other groups have evaluated the potentially heightened role of DCE sequences in disease localisation, they relied on TRUS-biopsy as a reference standard, rather than the gold-standard whole mount histology used in our study.^{18,20,21,35,36} The application of DCE in those studies also generally resulted in higher sensitivity for intraprostatic disease detection, as demonstrated in our results. Abd-Alazeez et al and Kim et al reported favourable indicators for DCE when compared with DWI. Donati et al, Alonzo et al and Luzurier et al reported more equivocal findings.

LIMITATIONS

We acknowledge certain limitations in this study. Salvage prostatectomy is an uncommon procedure, requiring careful patient selection and our patient sample was inevitably small. A retrospective design was most practical in this case, as inclusion required whole mount prostatectomy specimens. Inclusion of a small number of cases imaged either elsewhere (two patients) or with an endorectal coil (four patients) introduced a degree of heterogeneity into the data set. However, technical factors were homogeneous in the vast majority and

Figure 7. Role of DCE, seminal vesicle: right SVI shows minimal restricted diffusivity on high b-value DWI (A) and ADC (B), but disease is clearly shown as an enhancing nodule on the DCE image (C). Inclusion of DCE significantly upstaged the tumour in this case. ADC, apparent diffusioncoefficient; DCE, dynamic contrast enhanced; DWI, diffusion-weighted imaging; SVI, seminal vesicleinvolvement

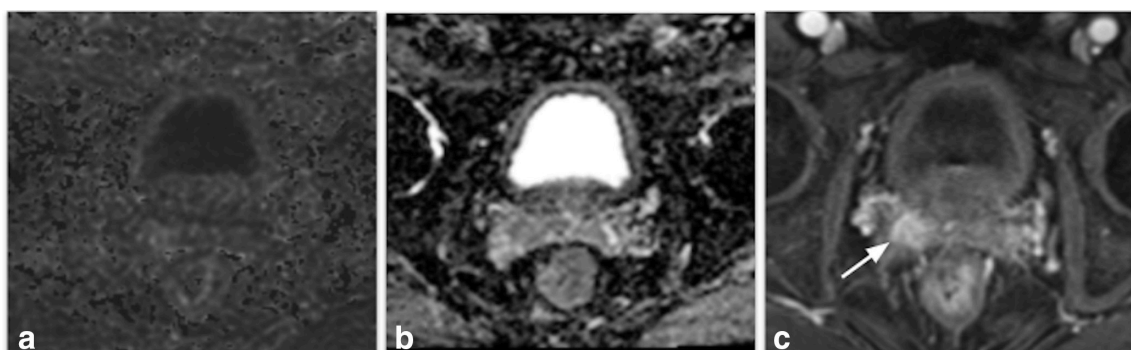


Table 4. Subgroup analysis with recalculated performance of MP-MRI, using DCE as a co-dominant sequence

	TP	FP	TN	FN	Sensitivity (%)	Specificity (%)
Intraprostatic disease, per hemi-gland (<i>n</i> = 34) PI-RADS v. 2						
Reader 1	14	0	7	13	52	100
Reader 2	19	1	6	8	70	86
Average					61	93
Intraprostatic disease, per hemi-gland (<i>n</i> = 34) Modified score						
Reader 1	18	1	6	9	67	86
Reader 2	23	1	6	4	85	86
Average					76	86

DCE, dynamic contrastenhanced; FN, false negative; FP, false positive; MP-MRI, multiparametric MRI; PI-RADS v. 2, Prostate Imaging-Reporting and Data System version 2; SVI, seminal vesicle involvement; TN, true negative; TP, true positive.

essential imaging protocols were compliant in all cases, and were unlikely to have had more than a minor impact on sensitivity and NPV. The inclusion of these cases also incorporates a limited amount of interinstitutional variance in referring centres, which is reflective of and translatable to current clinical practice and referral pathways.

As shown in Table 2, the interval between MRI and surgery was variable, with a median of 137.5 days. The majority of surgeries were performed under 6 months. In a generally indolent disease process, with limited alternative salvage options in this context, the central prostate MDT deemed the imaging to be applicable in surgical planning within a fairly broad time-frame. Six cases were notable outliers in this regard (*i.e.* time interval greater than 6 months), and this may have had a small impact on the overall radiological–pathological concordance.

Some authors have attempted radiological–pathological correlation by co-registering MRI regional maps with the multiple regions on TRUS-biopsy results. However, in our experience, reliable sublobar correlation of MRI detected lesions against template biopsy results or whole-mount pathology was not feasible. Conventional imaging sectoral scoring maps differ significantly from standard template biopsy regions and are not readily translatable. Differences between plane of image acquisition and orientation of whole-mount sections also confounds sectoral correlation with imaging. Hemi-gland analysis was therefore chosen as the most reliable means of radiological–pathological correlation for intraprostatic recurrence, and is sufficient to differentiate unilateral (\leq T2b) from bilateral (T2c) disease according to T-staging of disease according American Joint Committee on Cancer TNM staging.

CONCLUSION

In our cohort of patients, using PI-RADS v. 2, MP-MRI achieved high specificity and PPV, but only moderate sensitivity and low NPV for detecting radio-recurrent intraprostatic tumour and direct ECE. MP-MRI tends to under quantify and under stage locally recurrent prostate cancer. This should be acknowledged in the reporting of this imaging and allowed for in the surgical planning of these cases.

Introducing a modification to the overall MP-MRI scoring system, in which DCE was applied as a co-dominant sequence, resulted in a modest improvement in the overall diagnostic performance of MP-MRI, with an increased sensitivity and slightly decreased (but still high) specificity. Where possible, we therefore strongly recommend the use of DCE in the evaluation of suspected locally recurrent prostate cancer and we suggest an emphasis on DCE in any future consensus scoring system intended for this setting.

ACKNOWLEDGEMENTS

The research was supported by the National Institute for Health Research (NIHR) Royal Marsden Biomedical Research Centre and the NIHR Imperial Biomedical Research Centre. The views expressed are those of the authors and not necessarily those of the National Health Service, the NIHR or the Department of Health and Social Care.

FUNDING

No funding was received for conducting this study. The authors have no relevant financial or non-financial interests to disclose.

ETHICS APPROVAL

Ethical approval was waived by the local Ethics Committee in view of the retrospective nature of the study and all procedures being performed were part of routine care.

REFERENCES

- Van den Broeck T, van den Bergh RCN, Arfi N, Gross T, Moris L, Briens E, et al. Prognostic value of biochemical recurrence following treatment with curative intent for prostate cancer: a systematic review. *Eur Urol* 2019; **75**: 967–87. doi: <https://doi.org/10.1016/j.eururo.2018.10.011>
- Coakley FV, Hricak H, Wefer AE, Speight JL, Kurhanewicz J, Roach M. Brachytherapy for prostate cancer: endorectal MR imaging of local treatment-related changes. *Radiology* 2001; **219**: 817–21. doi: <https://doi.org/10.1148/radiology.219.3.r01jn46817>
- Nudell DM, Wefer AE, Hricak H, Carroll PR. Imaging for recurrent prostate cancer. *Radiol Clin North Am* 2000; **38**: 213–29. doi: [https://doi.org/10.1016/S0033-8389\(05\)70157-3](https://doi.org/10.1016/S0033-8389(05)70157-3)
- Chan TW, Kressel HY. Prostate and seminal vesicles after irradiation: Mr appearance. *J Magn Reson Imaging* 1991; **1**: 503–11. doi: <https://doi.org/10.1002/jmri.1880010502>
- Mertan FV, Greer MD, Borofsky S, Kabakus IM, Merino MJ, Wood BJ, et al. Multiparametric magnetic resonance imaging of recurrent prostate cancer. *Top Magn Reson Imaging* 2016; **25**: 139–47. doi: <https://doi.org/10.1097/RMR.0000000000000088>
- Barchetti F, Panebianco V. Multiparametric MRI for recurrent prostate cancer post radical prostatectomy and postradiation therapy. *Biomed Res Int* 2014; **2014**: 1–23Epub 2014 May 25. doi: <https://doi.org/10.1155/2014/316272>
- McNeal JE, Redwine EA, Freiha FS, Stamey TA. Zonal distribution of prostatic adenocarcinoma. Correlation with histologic pattern and direction of spread. *Am J Surg Pathol* 1988; **12**: 897–906. doi: <https://doi.org/10.1097/00000478-198812000-00001>
- American College of RadiologyPI-RADSTM Prostate Imaging – Reporting and Data System version 2 [Internet]. 2015. Available from: <https://www.acr.org/-/media/ACR/Files/RADS/PI-RADS/PIRADS-V2.pdf> [cited 7 Nov 2020].
- American College of RadiologyPI-RADSTM Prostate Imaging – Reporting and Data System version 2.1 [Internet]. 2019. Available from: <https://www.acr.org/-/media/ACR/Files/RADS/PI-RADS/PIRADS-V2-1.pdf> [cited 7 Nov 2020].
- Haider MA, Chung P, Sweet J, Toi A, Jhaveri K, Ménard C, et al. Dynamic contrast-enhanced magnetic resonance imaging for localization of recurrent prostate cancer after external beam radiotherapy. *Int J Radiat Oncol Biol Phys* 2008; **70**: 425–30. doi: <https://doi.org/10.1016/j.ijrobp.2007.06.029>
- Rouvière O, Valette O, Grivolat S, Colin-Pangaud C, Bouvier R, Chapelon JY, et al. Recurrent prostate cancer after external beam radiotherapy: value of contrast-enhanced dynamic MRI in localizing intraprostatic tumor--correlation with biopsy findings. *Urology* 2004; **63**: 922–7. doi: <https://doi.org/10.1016/j.urology.2003.12.017>
- Roy C, Foudi F, Charton J, Jung M, Lang H, Saussine C, et al. Comparative sensitivities of functional MRI sequences in detection of local recurrence of prostate carcinoma after radical prostatectomy or external-beam radiotherapy. *American Journal of Roentgenology* 2013; **200**: W361–8. doi: <https://doi.org/10.2214/AJR.12.9106>
- Kara T, Akata D, Akyol F, Karçaaltıncaba M, Özmen M. The value of dynamic contrast-enhanced MRI in the detection of recurrent prostate cancer after external beam radiotherapy: correlation with transrectal ultrasound and pathological findings. *Diagn Interv Radiol* 2011; **17**: 38–43. doi: <https://doi.org/10.4261/1305-3825.DIR.3079-09.1>
- Tamada T, Sone T, Jo Y, Hiratsuka J, Higaki A, Higashi H, et al. Locally recurrent prostate cancer after high-dose-rate brachytherapy: the value of diffusion-weighted imaging, dynamic contrast-enhanced MRI, and T2-weighted imaging in localizing tumors. *AJR Am J Roentgenol* 2011; **197**: 408–14. doi: <https://doi.org/10.2214/AJR.10.5772>
- Kim CK, Park BK, Lee HM. Prediction of locally recurrent prostate cancer after radiation therapy: incremental value of 3T diffusion-weighted MRI. *J Magn Reson Imaging* 2009; **29**: 391–7. doi: <https://doi.org/10.1002/jmri.21645>
- Morgan VA, Riches SF, Giles S, Dearnaley D, deSouza NM. Diffusion-Weighted MRI for locally recurrent prostate cancer after external beam radiotherapy. *AJR Am J Roentgenol* 2012; **198**: 596–602. doi: <https://doi.org/10.2214/AJR.11.7162>
- Westphalen AC, Reed GD, Vinh PP, Sotto C, Vigneron DB, Kurhanewicz J. Multiparametric 3T endorectal MRI after external beam radiation therapy for prostate cancer. *J Magn Reson Imaging* 2012; **36**: 430–7. doi: <https://doi.org/10.1002/jmri.23672>
- Kim CK, Park BK, Park W, Kim SS. Prostate MR imaging at 3T using a phased-arrayed coil in predicting locally recurrent prostate cancer after radiation therapy: preliminary experience. *Abdom Imaging* 2010; **35**: 246–52. doi: <https://doi.org/10.1007/s00261-008-9495-2>
- Akin O, Gultekin DH, Vargas HA, Zheng J, Moskowitz C, Pei X, et al. Incremental value of diffusion weighted and dynamic contrast enhanced MRI in the detection of locally recurrent prostate cancer after radiation treatment: preliminary results. *Eur Radiol* 2011; **21**: 1970–8. doi: <https://doi.org/10.1007/s00330-011-2130-6>
- Donati OF, Jung SI, Vargas HA, Gultekin DH, Zheng J, Moskowitz CS, Hricak H, et al. Multiparametric prostate MR imaging with T2-weighted, diffusion-weighted, and dynamic contrast-enhanced sequences: are all pulse sequences necessary to detect locally recurrent prostate cancer after radiation therapy? *Radiology* 2013; **268**: 440–50. doi: <https://doi.org/10.1148/radiol.13122149>
- Alonzo F, Melodelima C, Bratan F, Vitry T, Crouzet S, Gelet A, et al. Detection of locally radio-recurrent prostate cancer at multiparametric MRI: can dynamic contrast-enhanced imaging be omitted? *Diagn Interv Imaging* 2016; **97**: 433–41. doi: <https://doi.org/10.1016/j.diii.2016.01.008>
- El-Shater Bosaily A, Parker C, Brown LC, Gabe R, Hindley RG, Kaplan R, et al. PROMIS--Prostate MR imaging study: A paired validating cohort study evaluating the role of multi-parametric MRI in men with clinical suspicion of prostate cancer. *Contemp Clin Trials* 2015; **42**: 26–40. doi: <https://doi.org/10.1016/j.cct.2015.02.008>
- Pucar D, Shukla-Dave A, Hricak H, Moskowitz CS, Kuroiwa K, Olgac S, et al. Prostate cancer: correlation of Mr imaging and MR spectroscopy with pathologic findings after radiation therapy-initial experience. *Radiology* 2005; **236**: 545–53. doi: <https://doi.org/10.1148/radiol.2362040739>
- Sala E, Eberhardt SC, Akin O, Moskowitz CS, Onyebuchi CN, Kuroiwa K, et al. Endorectal MR imaging before salvage prostatectomy: tumor localization and staging. *Radiology* 2006; **238**: 176–83. doi: <https://doi.org/10.1148/radiol.2381052345>
- Zattoni F, Kawashima A, Morlacco A, Davis BJ, Nehra AK, Mynderse LA, et al. Detection of recurrent prostate cancer after primary radiation therapy: an evaluation of the role of multiparametric 3T magnetic resonance imaging with endorectal coil. *Pract Radiat Oncol* 2017; **7**: 42–9. doi: <https://doi.org/10.1016/j.prro.2016.06.003>
- Altman D. *Practical statistics for medical research*. Chapman and. London: Hall; 1991.
- Dinis Fernandes C, Ghobadi G, van der Poel HG, de Jong J, Heijmink SWTPJ, Schoots I, et al. Quantitative 3-T multi-parametric MRI and step-section pathology of recurrent

- prostate cancer patients after radiation therapy. *Eur Radiol* 2019; **29**: 4160–8. doi: <https://doi.org/10.1007/s00330-018-5819-y>
28. Rosenkrantz AB, Ginocchio LA, Cornfeld D, Froemming AT, Gupta RT, Turkbey B, et al. Interobserver reproducibility of the PI-RADS version 2 lexicon: a multicenter study of six experienced prostate radiologists. *Radiology* 2016; **280**: 793–804. doi: <https://doi.org/10.1148/radiol.2016152542>
29. Girometti R, Giannarini G, Greco F, Isola M, Cereser L, Como G, et al. Interreader agreement of PI-RADS V. 2 in assessing prostate cancer with multiparametric MRI: a study using whole-mount histology as the standard of reference. *J Magn Reson Imaging* 2019; **49**: 546–55. doi: <https://doi.org/10.1002/jmri.26220>
30. Kasel-Seibert M, Lehmann T, Aschenbach R, Guettler FV, Abubrig M, Grimm M-O, et al. Assessment of PI-RADS V2 for the detection of prostate cancer. *Eur J Radiol* 2016; **85**: 726–31. doi: <https://doi.org/10.1016/j.ejrad.2016.01.011>
31. Park SY, Jung DC, Oh YT, Cho NH, Choi YD, Rha KH, et al. Prostate cancer: PI-RADS version 2 helps preoperatively predict clinically significant cancers. *Radiology* 2016; **280**: 108–16. doi: <https://doi.org/10.1148/radiol.16151133>
32. Purysko AS, Bittencourt LK, Bullen JA, Mostardeiro TR, Herts BR, Klein EA. Accuracy and interobserver agreement for prostate imaging reporting and data system, version 2, for the characterization of lesions identified on multiparametric MRI of the prostate. *AJR Am J Roentgenol* 2017; **209**: 339–49. doi: <https://doi.org/10.2214/AJR.16.17289>
33. Schiavina R, Ceci F, Borghesi M, Brunocilla E, Vagnoni V, Gacci M, et al. The dilemma of localizing disease relapse after radical treatment for prostate cancer: which is the value of the actual imaging techniques? *Curr Radiopharm* 2013; **6**: 92–5. doi: <https://doi.org/10.2174/1874471011306020005>
34. Rouvière O, Vitry T, Lyonnet D. Imaging of prostate cancer local recurrences: why and how? *Eur Radiol* 2010; **20**: 1254–66. doi: <https://doi.org/10.1007/s00330-009-1647-4>
35. Abd-Alazeez M, Ramachandran N, Dikaios N, Ahmed HU, Emberton M, Kirkham A, et al. Multiparametric MRI for detection of radiorecurrent prostate cancer: added value of apparent diffusion coefficient maps and dynamic contrast-enhanced images. *Prostate Cancer Prostatic Dis* 2015; **18**: 128–36. doi: <https://doi.org/10.1038/pcan.2014.55>
36. Luzurier A, Jouve De Guibert P-H, Allera A, Feldman SF, Conort P, Simon JM, et al. Dynamic contrast-enhanced imaging in localizing local recurrence of prostate cancer after radiotherapy: limited added value for readers of varying level of experience. *J Magn Reson Imaging* 2018; **48**: 1012–23. doi: <https://doi.org/10.1002/jmri.25991>